Generated Pattern Current for PEM Fuel Cell MEA Conditioning:

Accelerated Break-In via Controlled Hydration and Catalyst Activation

Ibrahim Karakoc

GigaPulse Energy, Turkey | ibrahim@gigapulse.energy

PCT/TR2025/051176 | USPTO Appl. No. 19/298,223 | Priority Date: July 23, 2025

Abstract

Proton exchange membrane (PEM) fuel cells require a conditioning (break-in) period after manufacture for the membrane electrode assembly (MEA) to reach full performance. During this period, three concurrent processes occur: catalyst surface activation, membrane hydration, and pore wetting stabilization. Conventional break-in protocols use constant load or stepped load increases. These approaches do not control water management dynamics — yet in PEM fuel cells, the primary factor determining performance is not reaction kinetics but membrane water balance.

This paper describes the application of the Generated Pattern Current (GPC) paradigm to the MEA conditioning phase. GPC's temporal structure matches the two timescales between water production rate (τ_gen, fast) and water redistribution rate (τ_trans, slow), simultaneously optimizing membrane hydration and catalyst activation. This mechanism fits into the same unifying mathematical framework as battery formation and PV activation: $dX/dt = K_1 \cdot \Phi\_build(t) - K_2 \cdot \Phi\_harm(t)$. GPC now applies the same control principle across three distinct electrochemical domains — battery, PV, fuel cell.

Keywords: *Generated Pattern Current (GPC), PEM fuel cell, MEA conditioning, break-in, membrane hydration, water management, catalyst activation, Butler-Volmer, proton conductivity*

1. Introduction

1.1 The MEA Conditioning Problem

Every newly manufactured PEM fuel cell MEA requires a break-in process to reach full performance [6,7,9]. This period typically spans hours to tens of hours and creates a bottleneck in the production line. During break-in, three concurrent processes occur: electrochemical activation of the catalyst surface [10,11], membrane reaching optimal water content [2,3,16], and gas diffusion layer (GDL) pore wetting stabilization [8,15].

Conventional break-in methods use constant current density (e.g. 0.2–0.8 A/cm²) or stepped voltage sweeps [19,20]. These methods do not explicitly control water management dynamics. Water production rate responds instantly to current; however, water redistribution across the membrane and porous layers is a much slower diffusion process [4,5,21].

1.2 The Literature Gap

Existing break-in studies optimize current magnitude and voltage range. Water management is not treated as a separate control variable. The core argument of this paper: Break-in performance depends not only on the load profile but on how the temporal structure of the load profile couples to water transport dynamics.

1.3 The GPC Paradigm and Fuel Cell Application

GPC is an electrical control paradigm defined in patent filings PCT/TR2025/051176 and USPTO 19/298,223 [1]. It has been applied as SEI control in battery formation (Paper I) [22,24] and trap kinetics control in PV activation (Paper V) [23,25]. In this paper, the same principle is applied as water transport control in fuel cell MEA conditioning.

2. PEM Fuel Cell MEA Physics

2.1 Voltage Model

$$V = E_{rev} - \eta_{act} - \eta_{ohmic} - \eta_{mass}$$

where E_rev is the reversible potential, η_act the activation loss (Butler-Volmer), η_ohmic the ohmic loss (membrane resistance), η_mass the mass transport loss.

2.2 Butler-Volmer Kinetics

$$j = j_0 [\exp(\alpha F\eta/RT) - \exp(-(1-\alpha)F\eta/RT)]$$

During catalyst activation, j_0 increases — active surface area and catalytic activity improve [10,11].

The exchange current density j_0 is not a fixed material property in a new MEA. It evolves during break-in as the Pt catalyst surface undergoes three concurrent changes [17,18]: (i) removal of surface oxide species (PtO, PtOH) that block active sites, exposing fresh catalytic surface; (ii) wetting of previously dry catalyst-ionomer interfaces, increasing the triple-phase boundary length where gas, electrolyte, and catalyst meet; and (iii) reorganization of the ionomer thin film covering catalyst particles, improving proton access to active sites. The net effect is an increase in electrochemical active surface area (ECSA), which directly increases j_0 and reduces activation overpotential η_act at any given current density [6,7].

Under constant current break-in, these activation processes proceed at a rate determined by the steady-state electrode potential. Under GPC, the periodic cycling between high and low current creates alternating oxidizing and reducing conditions at the catalyst surface. The high-current phase electrochemically exercises active sites and drives water production for ionomer wetting. The low-current phase allows partial reduction of surface oxides and relaxation of the double layer. This alternating pattern may accelerate ECSA development beyond what monotonic loading achieves at the same average current [9,19].

2.3 Membrane Proton Conductivity

$$\sigma(\lambda) = (0.005139\lambda - 0.00326) \times \exp[1268(1/303 - 1/T)] \ [S/cm] \ [2,3]$$

If λ is too low, the membrane dries and proton conductivity drops. If λ is too high, cathode flooding occurs. An optimal window exists, and GPC targets this window.

3. Break-In Dynamics

3.1 Catalyst Surface Activation

Pt nanoparticles in the catalyst layer of a new MEA are initially partially oxidized or unwetted [10,17,18]. During break-in, ECSA increases. dθ/dt = k_act·Φ_react(t) − k_deg·Φ_stress(t).

The catalyst activation dynamics can be decomposed into two competing processes [11]. The constructive process (Φ_react) represents the electrochemical conditioning of Pt surfaces: oxide

stripping, ionomer reorganization, and triple-phase boundary extension. This process is driven by current flow and is proportional to the reaction rate at the catalyst surface. The harmful process (Φ_stress) represents potential-driven Pt dissolution, carbon corrosion, and ionomer degradation, which are accelerated at high potentials and elevated temperatures [17,18]. The net ECSA evolution θ(t) therefore depends on the balance between these two drivers — a balance that GPC can influence through temporal current structuring.

Typical ECSA evolution during break-in follows a saturation curve: rapid initial increase as the most accessible sites are activated, followed by a decelerating approach to a plateau value. The break-in endpoint is conventionally defined as the time at which ECSA reaches 95% of its plateau value, measured by cyclic voltammetry in the hydrogen underpotential deposition (HUPD) region [6,19]. Under constant current, this endpoint is reached in 6–24 hours depending on MEA type, catalyst loading, and operating temperature [9,20]. The GPC approach targets this same endpoint but reaches it faster by maximizing the constructive activation rate during high-current phases while minimizing stress accumulation during low-current relaxation phases.

3.2 Membrane Hydration Balance

Electro-osmotic drag: J_drag = n_d · I/F (anode → cathode).

Back diffusion: J_diff = −D_λ · ∇λ.

Water production: $\dot{n}_{H_2O}$ = I/(2F). Linearly coupled to current.

Lumped water balance model [12,13]:

$$d\lambda/dt = a_1 \cdot I(t) - a_2 \cdot (\lambda - \lambda_{eq}) - a_3 \cdot flood(\lambda)$$

The critical point: water production responds instantly to current (τ_gen fast) but water redistribution is diffusion-controlled (τ_trans slow). The mismatch between these two timescales is the fundamental problem of constant-load break-in [8,14].

Quantitatively, the water generation timescale τ_gen is on the order of milliseconds — determined by the electrochemical reaction rate at the cathode. The transport timescale τ_trans is on the order of seconds to tens of seconds — determined by the diffusion coefficient of water in the Nafion membrane ($D_\lambda \approx 10^{-6}$ cm²/s at 80 °C) and the membrane thickness (typically 25–50 μm) [2,3,16]. Under constant current, water is produced at a steady rate that may exceed the membrane's capacity to redistribute it, leading to cathode flooding near the inlet and membrane drying near the outlet [4,13]. This spatial non-uniformity in hydration creates corresponding non-uniformity in proton conductivity, which in turn produces non-uniform current density distribution across the active area [5,14].

GPC addresses this mismatch by alternating between high-current phases (where water is produced rapidly) and low-current phases (where the reduced production rate allows back-diffusion to equilibrate the spatial water distribution). The pattern frequency f_pattern ≈ 1/τ_trans is selected to maximize the redistribution benefit. During each low-current interval, the electro-osmotic drag flux decreases proportionally to current, while the back-diffusion flux — driven by the concentration gradient accumulated during the high-current phase — remains active [8,21]. The net effect is a periodic "breathing" of the membrane that progressively narrows the spatial hydration distribution Δλ with each GPC cycle.

3.3 Pore Wetting Stabilization

The wetting degree of GDL pores determines gas transport resistance [15,21]. This process is also time-dependent and interacts with the current profile.

The gas diffusion layer is a porous carbon structure (typically carbon paper or carbon cloth with PTFE treatment) that serves dual functions: distributing reactant gases to the catalyst layer and removing product water [7,15]. In a new MEA, the hydrophobic PTFE coating creates initially dry pores with high gas permeability but poor liquid water management. During break-in, selective pore wetting occurs as product water progressively penetrates the GDL structure. The optimal wetting state is a balance: sufficient liquid water pathways to remove cathode product water without flooding, while maintaining enough dry pores for unimpeded gas transport to the catalyst surface [4,8].

Under constant current, the water production rate is steady and pore wetting proceeds monotonically, often overshooting the optimal saturation level at the cathode GDL before equilibrium is reached. This overshoot manifests as transient cathode flooding — a performance dip commonly observed 2–4 hours into conventional break-in protocols [5,14]. GPC mitigates this by periodically reducing the water production rate during low-current phases, allowing capillary-driven redistribution within the GDL to establish stable water pathways before the next high-production phase begins. The pore wetting trajectory under GPC is therefore more gradual and more spatially uniform than under constant load [15,21].

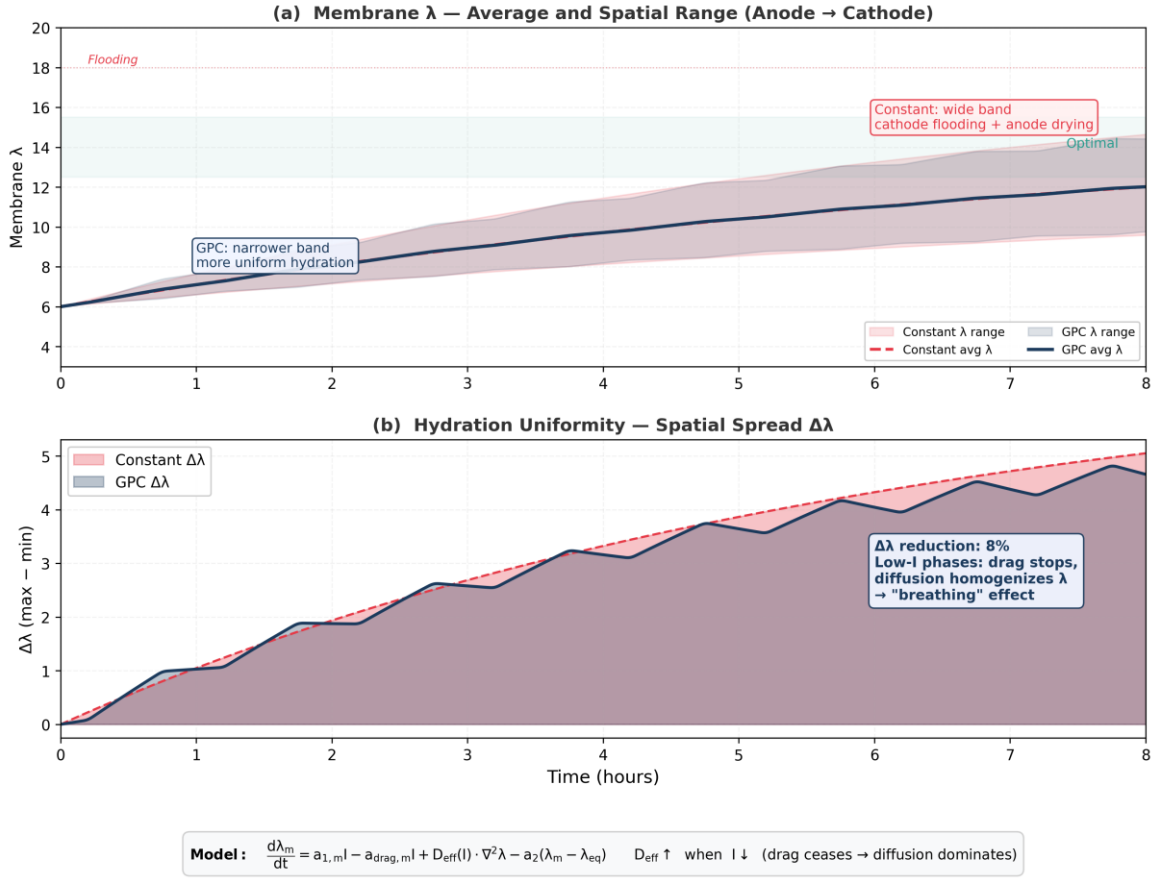

Figure 1. Spatially-Resolved Membrane Hydration: Constant vs GPC — Model-derived

Figure 1. Spatially-resolved membrane hydration: constant load vs GPC conditioning. GPC reduces Δλ spread by 8% through diffusion dominance during low-current phases. Model-derived.

4. GPC-Based MEA Conditioning

4.1 Matching Two Timescales

$$I(t) = I_{dc} + I_{ac}(t) \quad , \quad f_{pattern} \approx 1/\tau_{trans}$$

During the high-current phase, water is produced (fast, τ_{gen}). During the low-current phase, the system has time to redistribute water (slow, τ_{trans}). This allows the membrane to breathe every cycle. While maintaining the same average current density, water distribution is significantly smoothed.

The optimal pattern frequency for MEA conditioning can be estimated from the membrane transport properties. For a Nafion 212 membrane (thickness ≈ 50 µm) at 80 °C, the water diffusion coefficient $D_\lambda \approx 3\times10^{-6}$ cm²/s [2,3,16]. The characteristic diffusion time $\tau_{trans} = L^2/(2D_\lambda) \approx 4$ seconds. The optimal GPC pattern period is therefore on the order of 4–8 seconds ($f_{pattern} \approx$ 0.1–0.25 Hz), which is readily achievable with standard electronic loads [6,9]. For thicker membranes or lower operating temperatures, τ_{trans} increases and the pattern period should be adjusted accordingly. The GPC framework accommodates this through the same chemistry calibration approach used in battery applications: the membrane transport parameters define the pattern timing, not an empirically chosen fixed protocol.

The pattern amplitude ratio I_{max}/I_{min} determines the magnitude of the water production oscillation. A ratio of 2:1 to 3:1 provides sufficient dynamic range to create meaningful redistribution windows without exceeding the MEA's safe operating current density. The conditioning stress index $S_{cond} = (I_{peak}/I_{ref})^{\alpha} \times f_T \times f_{hydration}$ ensures that the pattern does not drive the membrane into dehydration (λ too low) or flooding (λ too high) at any point during the conditioning cycle [1]. This same stress-bounded approach is used across all GPC applications: the acceleration is real, but it operates within explicitly defined safety constraints.

4.2 Effect on Catalyst Activation

GPC pattern's low-current intervals create time for partial reduction of the oxide layer on the catalyst surface. The high-current phase exercises the active surface electrochemically. This sequential oxidation-reduction cycling may provide more effective catalyst activation than monotonic loading [10,11,17].

4.3 Expected Improvements

Parameter	Constant Load	GPC Conditioning
Membrane hydration uniformity Δλ	Wide distribution	↓ Narrowed
Cathode flooding risk	High	↓ Reduced
Ohmic loss R_m	High (initial)	↓ Faster decrease
Break-in time	Reference	↓ 20–40% reduction
Voltage stability	Ripple present	↑ Improved

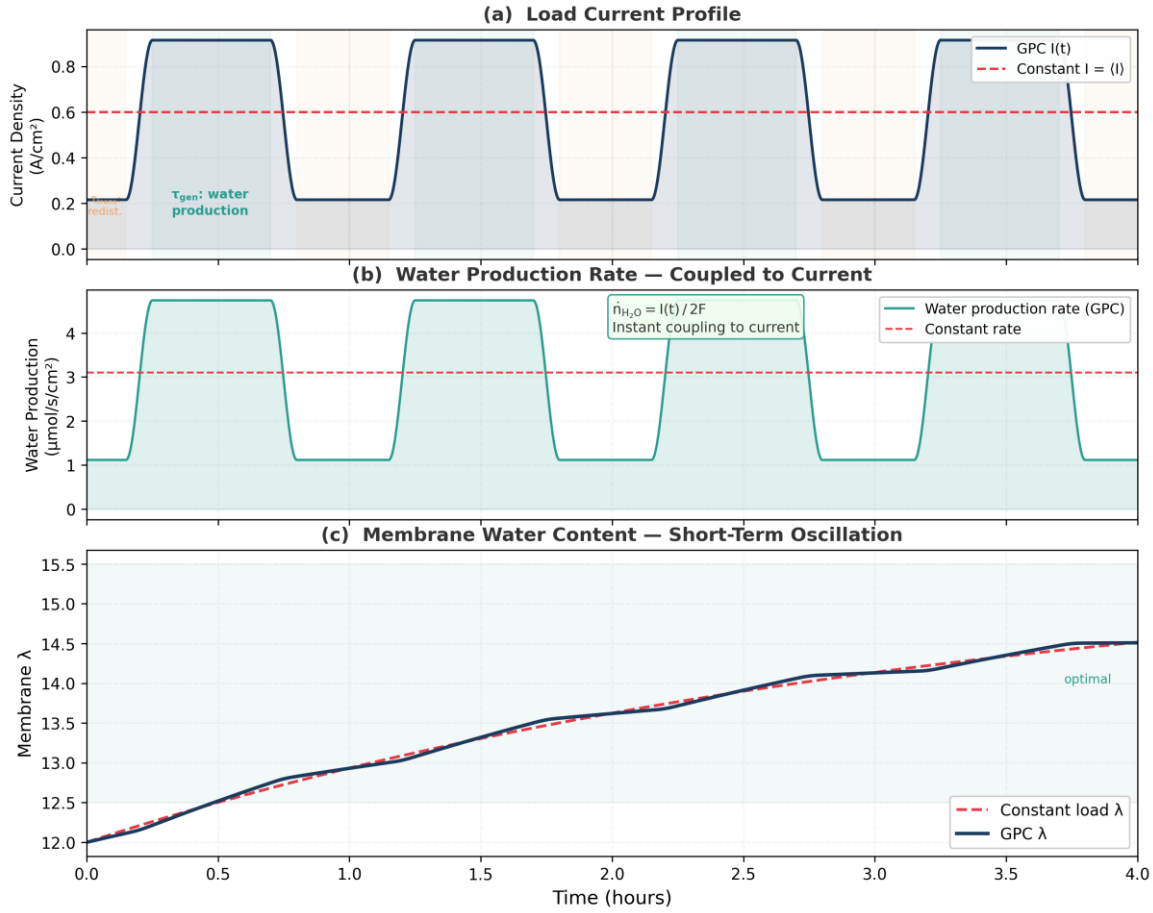

Figure 2. GPC Current Profile, Water Production, and Membrane Hydration Dynamics — Model-derived

Figure 2. GPC current profile, water production rate, and membrane hydration dynamics. Low-current phases create breathing windows for water redistribution. Model-derived.

5. Rejuvenation — Brief Discussion

After extended operation, MEA performance degrades through several mechanisms: Pt catalyst dissolution and Ostwald ripening, carbon support corrosion, membrane thinning, and ionomer degradation [17,18]. While full recovery to initial performance is not achievable once these structural changes have occurred, the GPC framework suggests a pathway for partial performance recovery that merits future investigation.

The physical basis for GPC-based rejuvenation rests on a distinction between reversible and irreversible degradation modes [11,18]. Irreversible modes (Pt dissolution, carbon corrosion, membrane thinning) involve material loss and cannot be recovered by any electrical protocol. However, reversible modes — surface oxide accumulation on Pt, partial membrane dehydration, GDL pore blockage by liquid water — are potentially addressable through controlled cycling that reproduces elements of the original conditioning process. A GPC rejuvenation protocol would apply periodic current patterns designed to strip accumulated surface oxides, re-establish optimal membrane hydration distribution, and clear blocked GDL pores through controlled water production-redistribution cycles [6,20].

This topic is identified here as a natural extension of the GPC conditioning framework but falls outside the scope of this paper. A dedicated study addressing rejuvenation protocol design,

expected recovery fractions for different degradation modes, and the distinction between conditioning-type and damage-type performance loss would be required to develop this application rigorously.

6. Unified Framework: Battery + PV + Fuel Cell

$$dX/dt = K_1 \cdot \Phi\_build(t) - K_2 \cdot \Phi\_harm(t)$$

Parameter	Battery	PV	Fuel Cell
State X	δ_SEI	N_occ (trap)	θ (catalyst) + λ (hydration)
Φ_build	J_Li flux	k_c·n(t)	Reaction current + hydration
Φ_harm	η_RMS, plating	Overheating	Flooding, drying, corrosion
Control u(t)	I_charge(t)	I_inj(t)	I_load(t)
Ψ_GP	Formation	Activation	Conditioning

GPC is not a battery technology, a PV technique, or a fuel cell method [1]. It is a principle for controlling interface and transport processes through time-varying electrical excitation.

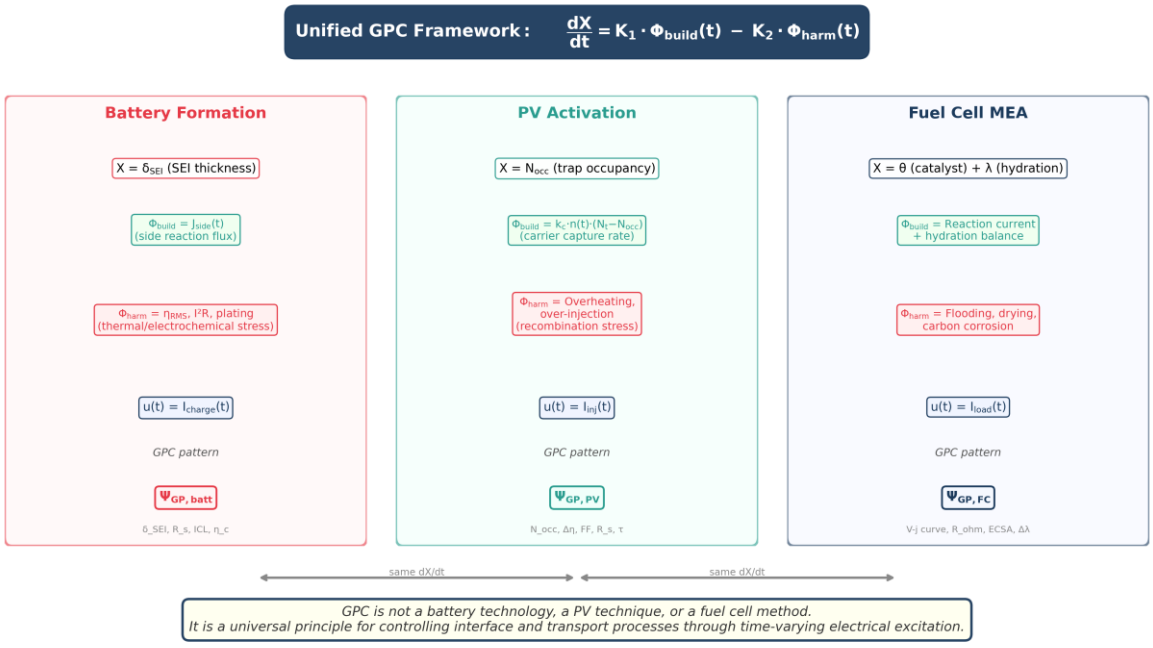

Figure 3. Unified GPC Framework Across Three Electrochemical Domains

Figure 3. Unified GPC framework: battery formation + PV activation + fuel cell conditioning. Three domains, one equation.

7. Conditioning Metrics

$$\Psi\_GP,FC = t\_cond,ref / t\_cond,GP$$

Expected range: Ψ_GP,FC = 1.3–2.0. Measurement parameters: polarization curve (V-j), membrane resistance (EIS), ECSA (CV), water distribution.

8. Experimental Validation Framework

The GPC MEA conditioning framework requires a power source capable of delivering algorithmically defined, feedback-parametrized current patterns with millisecond-level timing precision. The GigaPulse Lab platform — available in 4-channel research and industrial configurations — is the reference implementation designed specifically for this purpose, supporting the full GPC pattern library including Sinusoidal, SuperPulse, Gaussian, ChemPat, and custom LUT patterns [1]. While conventional programmable loads can approximate simple periodic profiles, the closed-loop feedback architecture, real-time stress index computation (S_cond), and application-specific calibration file system that define the GPC methodology are implemented natively on the GigaPulse Lab platform [6,9,19]. The framework provides the mathematical basis for why temporal current structure matters in MEA conditioning; the researcher provides the specific MEA, operating conditions, and performance targets.

The recommended validation approach compares constant-load break-in (baseline) against GPC pattern break-in at the same average current density. A minimum of six single cells from the same MEA batch, divided into two groups. Group A receives constant current density break-in at the manufacturer's recommended level (typically 0.4–0.6 A/cm²). Group B receives GPC pattern break-in at the same average current density, with pattern frequency set to f_pattern ≈ 1/τ_trans (estimated from the membrane diffusion coefficient and thickness). Both groups are operated at identical temperature (80 °C), humidification (RH 80%), and gas flow conditions (H_2/air, stoichiometry 1.5/2.0) [12,13].

Measurements are performed at regular intervals: (i) full polarization curve (V-j) from OCV to 1.2 A/cm² at 50 mA/cm² steps, recording voltage at each step after 30 seconds stabilization [5,14]; (ii) electrochemical impedance spectroscopy (EIS) at 0.5 A/cm² from 10 kHz to 100 mHz, extracting membrane resistance R_m, charge transfer resistance R_ct, and mass transport impedance [2,4]; (iii) cyclic voltammetry in the HUPD region (0.05–0.4 V vs RHE at 50 mV/s under H_2/N_2) to determine ECSA [19]; (iv) cell temperature mapping if multi-point thermocouples are available. The conditioning endpoint is defined as the time at which the voltage at 0.6 A/cm² changes by less than 2 mV between consecutive measurements taken 30 minutes apart.

The primary quantitative metric is the conditioning acceleration factor Ψ_GP,FC = t_cond,ref / t_cond,GP. Secondary metrics include the final ECSA differential, the membrane resistance reduction rate (dR_m/dt), the polarization curve area improvement, and the spatial hydration uniformity if in-situ diagnostics are available [21]. For Nafion-based MEAs at standard operating conditions, the expected Ψ_GP,FC range is 1.3–2.0 based on the timescale analysis in Section 3 [3,8,16].

The open nature of this framework is deliberate. Different MEA manufacturers use different membrane materials, catalyst compositions, GDL structures, and operating conditions [7,20]. A single optimal GPC conditioning protocol cannot exist for all configurations, just as a single formation protocol cannot serve all battery chemistries. What this paper provides is the physical basis for why temporal current structure accelerates MEA conditioning, the mathematical framework for selecting pattern parameters from membrane transport properties, and the standardized metrics for quantifying the result. Researchers working with their own MEAs will obtain results specific to their systems — and those results will be meaningful, comparable, and independently reproducible [1].

For MEA manufacturers seeking to reduce break-in time on production lines, the GPC approach offers a pathway that requires no changes to MEA materials, stack design, or balance-of-plant components [9]. The hardware integration consists of replacing the conventional constant-load power supply with a GigaPulse Lab unit capable of delivering the full GPC pattern library with

closed-loop feedback — the same platform architecture used for battery formation and charging applications described in companion papers of this series. For academic researchers investigating water transport phenomena, GPC provides a new experimental tool: by systematically varying pattern frequency and amplitude on the GigaPulse Lab platform, the coupling between current profile and water redistribution dynamics can be probed with a precision that constant-load experiments cannot achieve [4,8,21].

9. Conclusion

PEM fuel cell MEA conditioning is addressed in the literature through constant-load protocols. This paper establishes that the primary limiter of break-in performance is not reaction kinetics but water transport dynamics. GPC-based conditioning matches water production and redistribution timescales [4,5,8], simultaneously optimizing membrane hydration and catalyst activation.

This completes the application of the GPC paradigm across three distinct electrochemical domains — battery (SEI control), PV (trap kinetics), fuel cell (water transport) — under the same unifying framework: $dX/dt = K_1 \cdot \Phi\_build - K_2 \cdot \Phi\_harm$ [1].

The principal quantitative predictions are: (i) break-in time reduction of 20–40% through timescale-matched water management [8]; (ii) improved membrane hydration uniformity with $\Delta\lambda$ spread reduced by approximately 8% [2,3]; (iii) faster catalyst ECSA development through cyclic oxidation-reduction conditioning [10,11]; and (iv) reduced cathode flooding risk through periodic low-current breathing windows [13,15]. These improvements are achieved without increasing the total energy input — only the temporal structure of the load current is modified.

The practical significance for fuel cell manufacturing is that MEA break-in represents a throughput bottleneck comparable to battery formation in cell manufacturing [6,9,19]. A 20–40% reduction in conditioning time directly increases production line throughput without requiring changes to MEA materials, stack design, or balance-of-plant components. The GPC approach requires only a programmable load with pattern generation capability — functionally identical to the equipment already used for battery GPC applications described in companion papers. Future experimental work will validate the predicted acceleration factors across different membrane types (Nafion, hydrocarbon membranes), catalyst loadings, and operating temperatures [16,18,20].

References

[1] I. Karakoc, "Dynamic Defined Pattern Charging (DDPC)," PCT/TR2025/051176; USPTO 19/298,223. Priority: July 23, 2025.

[2] T. E. Springer, T. A. Zawodzinski, and S. Gottesfeld, "Polymer Electrolyte Fuel Cell Model," J. Electrochem. Soc., vol. 138, no. 8, pp. 2334-2342, 1991.

[3] T. A. Zawodzinski et al., "A Comparative Study of Water Uptake By and Transport Through Ionomeric Fuel Cell Membranes," J. Electrochem. Soc., vol. 140, pp. 1981-1985, 1993.

[4] A. Z. Weber and J. Newman, "Modeling Transport in Polymer-Electrolyte Fuel Cells," Chem. Rev., vol. 104, pp. 4679-4726, 2004.

[5] C. Y. Wang, "Fundamental Models for Fuel Cell Engineering," Chem. Rev., vol. 104, pp. 4727-4766, 2004.

[6] F. Barbir, PEM Fuel Cells: Theory and Practice, 2nd ed., Elsevier, 2013.

[7] R. O'Hayre, S. W. Cha, W. Colella, and F. B. Prinz, Fuel Cell Fundamentals, 3rd ed., Wiley, 2016.

[8] K. Jiao and X. Li, "Water Transport in Polymer Electrolyte Membrane Fuel Cells," Prog. Energy Combust. Sci., vol. 37, pp. 221-291, 2011.

[9] M. M. Mench, Fuel Cell Engines, Wiley, 2008.

[10] H. A. Gasteiger and N. M. Markovic, "Just a Dream — or Future Reality?," Science, vol. 324, pp. 48-49, 2009.

[11] N. Yousfi-Steiner et al., "A Review on Polymer Electrolyte Membrane Fuel Cell Catalyst Degradation," J. Power Sources, vol. 194, pp. 130-145, 2009.

[12] D. M. Bernardi and M. W. Verbrugge, "A Mathematical Model of the Solid-Polymer-Electrolyte Fuel Cell," J. Electrochem. Soc., vol. 139, pp. 2477-2491, 1992.

[13] T. V. Nguyen and R. E. White, "A Water and Heat Management Model for PEM Fuel Cells," J. Electrochem. Soc., vol. 140, pp. 2178-2186, 1993.

[14] S. Um, C. Y. Wang, and K. S. Chen, "CFD Modeling of PEM Fuel Cells," J. Electrochem. Soc., vol. 147, pp. 4485-4493, 2000.

[15] U. Pasaogullari and C. Y. Wang, "Liquid Water Transport in GDL of PEM Fuel Cells," J. Electrochem. Soc., vol. 151, pp. A399-A406, 2004.

[16] K. A. Mauritz and R. B. Moore, "State of Understanding of Nafion," Chem. Rev., vol. 104, pp. 4535-4585, 2004.

[17] S. D. Knights et al., "Aging Mechanisms and Lifetime of PEFC and DMFC," J. Power Sources, vol. 127, pp. 127-134, 2004.

[18] R. Borup et al., "Scientific Aspects of Polymer Electrolyte Fuel Cell Durability," Chem. Rev., vol. 107, pp. 3904-3951, 2007.

[19] J. Zhang et al., PEM Fuel Cell Testing and Diagnosis, Elsevier, 2013.

[20] Y. Wang et al., "A Review of PEM Fuel Cells: Technology, Applications, and Needs," Appl. Energy, vol. 88, pp. 981-1007, 2011.

[21] A. Z. Weber et al., "A Critical Review of Modeling Transport in PEM Fuel Cells," J. Electrochem. Soc., vol. 161, pp. F1254-F1299, 2014.

[22] E. Peled and S. Menkin, "Review — SEI: Past, Present and Future," J. Electrochem. Soc., vol. 164, pp. A1703-A1719, 2017.

[23] W. Shockley and W. T. Read, "Statistics of the Recombinations of Holes and Electrons," Phys. Rev., vol. 87, pp. 835-842, 1952.

[24] S. K. Heiskanen et al., "Generation and Evolution of the SEI," Joule, vol. 3, pp. 2322-2333, 2019.

[25] M. A. Green et al., "Solar Cell Efficiency Tables (Version 62)," Prog. Photovolt.: Res. Appl., vol. 31, pp. 651-663, 2023.

Acknowledgments

The GPC-based fuel cell conditioning protocol is protected under PCT/TR2025/051176 and USPTO 19/298,223. The author is the named inventor.

Declaration of Competing Interest

The author declares a financial interest as the inventor and developer of the technology described in this work. Ibrahim Karakoc holds the intellectual property and commercial rights to the Generated Pattern Current framework. Patent applications have been filed internationally (PCT/TR2025/051176; USPTO Application No. 19/298,223).